

AN OVERALL LTCC PACKAGE SOLUTION FOR X-BAND TILE T/R MODULE

Zhong-Jun Yu*, Zheng Xu, Yun-Kai Deng,
and Zhi-Guang Zhang

Institute of Electronics, Chinese Academy of Sciences, Beijing 100190, China

Abstract—An overall Low-Temperature Co-fired Ceramics (LTCC) package solution for X-band T/R module has been presented in this paper. This tile type package contributes to a dramatic reduction in size and weight of the T/R module. Moreover, an obvious merit of ceramic housing is better consistency of Coefficient of Thermal Expansion (CTE), compared with the traditional combination of ceramic board and metal housing. The schematic diagram and 3-D structure of the T/R module have been presented and a novel vertical interconnection based on Ball Grid Array (BGA) has been proposed to connect vias in the lid and those in the stage of the main LTCC pan. The LTCC T/R module has been fabricated and measured. It is compact in size ($20 \times 20 \times 2.6 \text{ mm}^3$) and has a weight of 3.5 g. The measured transmit output power is $33 \pm 1 \text{ dBm}$ in the frequency range from 8.8 GHz to 10.4 GHz, and the measured receive gain and Noise Figure are 29–30.5 dB and 2.6–2.8 dB, respectively.

1. INTRODUCTION

Phased array radar has versatile performance and has been widely applied in civilian and military missions. In the extensive applications, a phased array radar system consists of thousands of Transmit/Receive (T/R) modules. The cost, weight, and volume of the phased array radar are mainly related to T/R modules [1]. Therefore it is indispensable to do research on low-cost, low-weight, and compact T/R module. Low Temperature Co-fired Ceramics (LTCC) provide a 3-D circuit design method [2] and a great many microwave and millimeter wave components and devices have been researched and realized [3].

Received 10 January 2013, Accepted 4 March 2013, Scheduled 20 March 2013

* Corresponding author: Zhong-Jun Yu (speed_yzj@sohu.com).

Tile type T/R module adopting overall LTCC package solution shows an advantage in reducing weight and volume compared with traditional metal-sheltered LTCC board [4]. To realize the compact T/R module mentioned, it has to achieve specific requirements, such as vertical interconnection and efficient integration. Seldom there are reports on compact X-band LTCC T/R module. In a published case, although the X-band MMIC receiver front-end is compact receive gain needs to be improved [5].

In this paper, an overall LTCC package solution for X-band T/R module is presented. The system and structure of the T/R module is provided and a novel vertical interconnection taking advantage of Ball Grid Array (BGA) is proposed to connect vias in the lid and those in the stage of the main LTCC pan. Based on the prototype, a LTCC T/R module of 8.8–10.4 GHz has been fabricated and measured. Test result reveals that the T/R module delivers a remarkable performance while maintaining tiny and compact. It shows promise in diverse applications in addition to phased array radar. The LTCC tile with vertical RF feed is quite suitable for smart antenna use [6, 7], and the low weight feature allows it to be mounted on small UAV for agile missions [8].

2. SYSTEM OVERVIEW

The schematic diagram of the T/R module is shown in Figure 1. The whole function circuits except for the control unit are realized by five GaAs MMICs, including core chip, serial to parallel chip, Power Amplifier (PA) chip, Low Noise Amplifier (LNA) chip and switch chip. They are connected with microstrip as well as bond wires.

To reduce the size of the T/R module, both 6-bit phase shifter and 6-bit attenuator are integrated in the core chip, as shown in Figure 1.

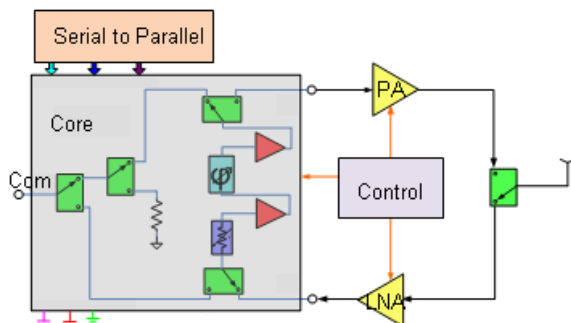


Figure 1. Schematic diagram of the X-band T/R module.

Switches inside the core chip and a switch next to the antenna operate together to alter between transmit mode and receive mode.

In transmit mode, the switches inside core chip routes the signal from the common port to PA, then from PA to antenna. While in receive mode, signals received by antenna are routed from LNA to core chip, then to the common port. As for the control unit, FPGA generates control signals, and they are routed to the manifold on the bottom of the T/R module.

All MMICs are mounted inside a hermetic box using LTCC processes. The hermetic housing not only protects vulnerable and friable MMICs from outer pollution and scratch, but also works as a shielding cavity for a single T/R module. As shown in Figure 2, to obtain a compact LTCC T/R module, LTCC is employed to design both side walls and board of the housing, resulting into an overall ceramic pan. And at the radiating end a stage is reserved in the cavity for vertical interconnection of signals.

The lid of the housing is also fabricated by LTCC processes, the same technique as that of the pan. There is benefit for a high level of consistency and efficiency on manufacturing.

Kovar provides a CTE compliant with ceramics. For this reason a Kovar frame is fabricated as the seal ring, which conjoins ceramic pan and lid mentioned above, shown in Figure 2. As for RF signal feeding

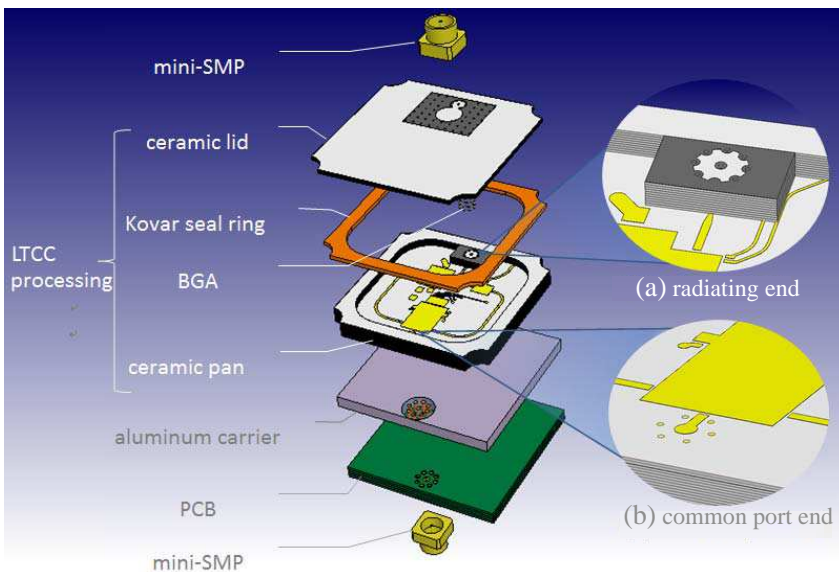


Figure 2. Structure of the LTCC T/R module.

between the pan and the lid, BGA (Ball Grid Array) is adopted. The central ball routes RF signal while outer balls serve as coax-like GND. By the way, the height of Kovar seal ring is fabricated slightly less than the diameter of BGA balls. Thus BGA balls are able to contact with lid and pan effectively.

At the common port end, RF signal carried by microstrip is fed down to bottom of the ceramic pan through a quasi-coaxial structure, which is formed by a central RF via and six outer shield vias. Beneath the ceramic pan there locates an aluminum carrier, in which a quasi-coaxial structure is embedded. This quasi-coaxial structure is formed by fuzz buttons embedded in a FR4 cylinder. Beneath the aluminum carrier there locates the PCB (Printed Circuit Board). Another quasi-coaxial structure is formed by vias in the PCB. These three quasi-coaxial structures interconnect together to let through RF signals. In the end, a mini-SMP is mounted upside-down on the PCB to supply an interface to the common port end. Actually there are many scattered vias in the ceramic pan, aluminum carrier (embedded in sheltering FR4 cylinder) and PCB which serves to supply power and route control signals vertically. They are not shown in the illustration for a clear view.

3. VERTICAL INTERCONNECTION DESIGN

The challenge of proposed tile package solution is mainly on vertical interconnections. At the very end of vertical interconnection, mini-SMP is adopted to supply an interface while maintaining a compact size. As for mini-SMP, detailed parameters have been provided by the manufacturer [9]. Return loss is greater than 26 dB at X band, and insertion loss is less than $0.1 \times \sqrt{f}$, which is about 0.3 dB in this case. Such an insertion loss is qualified in this work.

As for vertical interconnection at the radiating end, three quasi-coaxial structures are designed, i.e., in the lid (Figure 3(b)), in the stage (Figure 3(a)) and the other constructed by BGA balls. Dimension of the quasi-coaxial structure imitates that of coaxial structure, thus 50 Ohm match impedance is achieved [10].

The LTCC green tape employed here is 0.094 mm thick each layer after sintering, which possesses a dielectric constant of 5.9. The lid is made of 5 layers, and the ceramic pan is made of 22 layers with top 10 layers excavated to form a cavity and a stage. Top of the stage is partially plated to form a ground plane with clearance around inner RF path (Figure 3). At the same time 2 layers below the stage there locates a ground plane. It serves as the GND of microstrip lines distributed inside the cavity routing signals among MMICs.

The quasi-coaxial structures in the lid and that in the stage share the same dimension. Seven vias construct outer shield with a diameter D_o (1.8 mm) and inner via possess a diameter D_i (0.254 mm). Then BGA is adopted to connect vias in the lid and those in the stage of the ceramic pan. Every single BGA ball possesses a diameter of 0.5 mm.

When microstrip line routes into the stage, it changes into stripline (Figure 3(a)). Width of the microstrip W_{MS} is 0.28 mm. The stripline is actually offset strip transmission line, since the distance between the stripline and ground plane on top of the stage (10 layers) is not the same as that between the stripline and internal ground plane (2 layers). Width of the offset strip transmission line W_{SL} is initially calculated according to [11]. Then it is moderately tuned and set to 0.13 mm since upper GND of the offset stripline is not perfect. A taper is located between stripline and microstrip for smooth transition thus energy reflection is reduced [12]. Length of the taper L_{tp} is set to be 0.5 mm.

The whole RF path at the radiating end, i.e., from top of the lid down to end of the microstrip in the cavity is simulated by HFSS software. Simulation results are show in Figure 4. The insertion loss is better than 0.1 dB and Standing Wave Ratio (SWR) is less than 1.14. According to simulation results, the vertical interconnection at the radiating end is adequate for use.

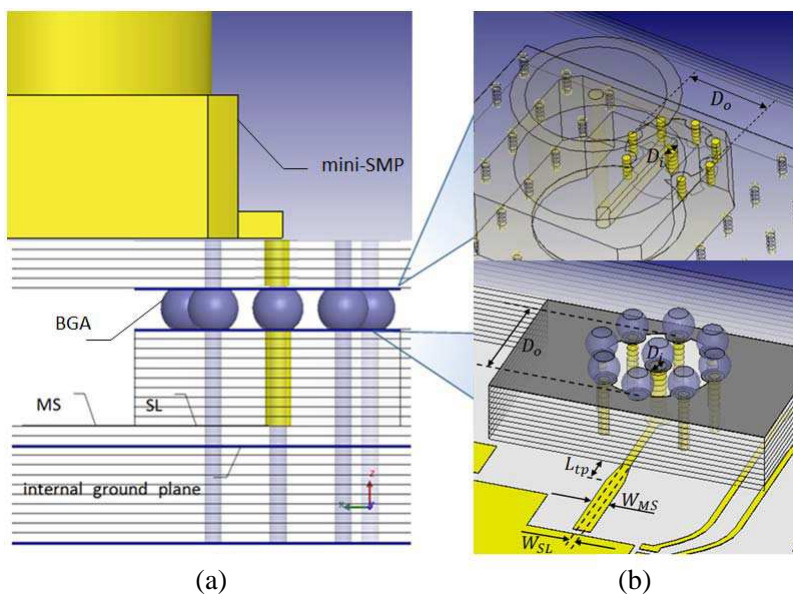


Figure 3. Vertical interconnection at the radiating end.

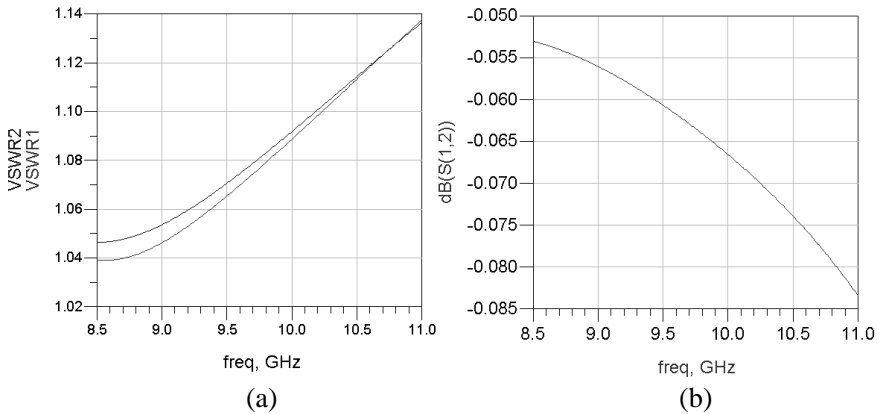


Figure 4. Simulation results of interconnection at the radiating end. (a) VSWR. (b) Insertion Loss.

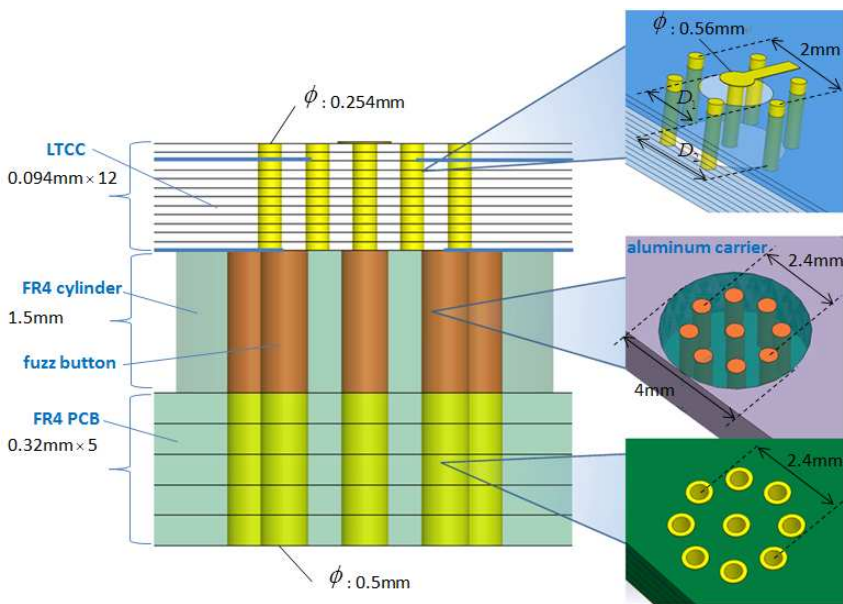


Figure 5. Vertical interconnection at the common port end.

Another interconnection requiring evaluation is that of the common port end (Figure 5). Three quasi-coaxial structures exist here. RF signal traveling along the microstrip is vertically fed down through the ceramic pan. An inner via and six outer shield vias construct a quasi-coaxial structure. All of these vias in the ceramic pan possess a

diameter of 0.254 mm. The diameter of outer shield ring is 2 mm.

Clearance are made on GND planes where RF via pass through. Diameter of clearance in the GND beneath the ceramic pan (D_2) is preset to be 1.8 mm, thus diameter of clearance in the internal GND (D_1) has to be elaborately adjusted to get 50 Ohm characteristic impedance [13].

At the bottom of the ceramic pan, i.e., the bottom of the tile T/R module, RF vias are pressed with fuzz buttons. The fuzz buttons are embedded in a FR4 cylinder, the same material with that of the PCB beneath. The quasi-coaxial structures in the FR4 cylinder and that in the PCB share the same dimension. Elasticity of fuzz button brings about an effective contact with LTCC T/R module and PCB [14].

Vertical interconnection at the common port end is simulated in HFSS. All of the components illustrated in Figure 5 are included. In Figure 6, simulation result shows the structure in Figure 5 has an insertion loss less than 0.2 dB, while its SWR is about 1.2. From the simulation results in Figures 4 and 6, a conclusion is drawn that vertical transitions presented in this paper are capable in the design of LTCC T/R module.

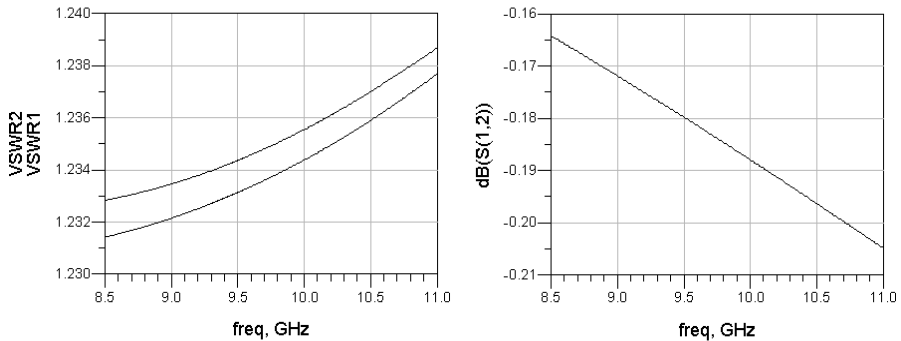


Figure 6. Simulation results of interconnection at the common port end.

4. FABRICATION AND MEASUREMENTS

The fabricated X-band LTCC T/R module is shown in Figure 7. The T/R module has a compact size of $20 \times 20 \times 2.6 \text{ mm}^3$ (without mini-SMP connector), and has a weight of 3.5 g, including mounted MMICs and mini-SMP connector. In the future work, after the present lid with mini-SMP is replaced with smart antenna, the weight can be reduced further.

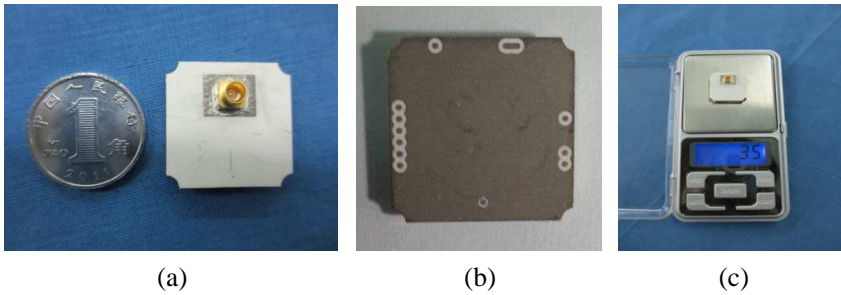


Figure 7. Fabricated X-band LTCC T/R module. (a) Front view. (b) Bottom view. (c) Weight measurement of the T/R module.

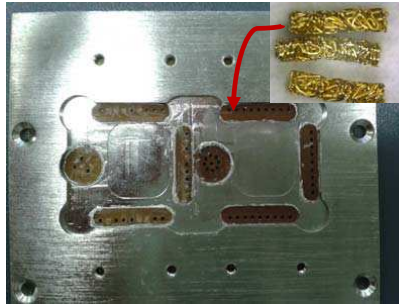


Figure 8. Aluminum carrier with fuzz buttons embedded.

As shown in Figure 7(b), bottom of the T/R module is etched to distribute RF and DC pads. These pads are pressed with fuzz button to test the fabricated LTCC T/R module. In this demonstrator, fuzz buttons are embedded in FR4 bricks. After enclosed with thin metal foil, FR4 bricks are then embedded in an aluminum carrier which is plated with Ni in Figure 8. The bottom side of the carrier is pressed with PCB. When performing tests with the carrier, an indium slice on the carrier where PA locates is recommended for better heat dissipation.

In addition, a test vehicle is specially designed and fabricated for this X-band LTCC T/R module, as shown in Figure 9. The vehicle provides the feed of RF signal, bias voltage and control logic. Tile T/R module is fixed by test jigs. The test vehicle can test two tile modules simultaneously.

Measurement of output power in transmit mode is performed by connecting the common port end to Agilent E8257D signal generator and connecting the radiating end to Agilent N1912A power meter

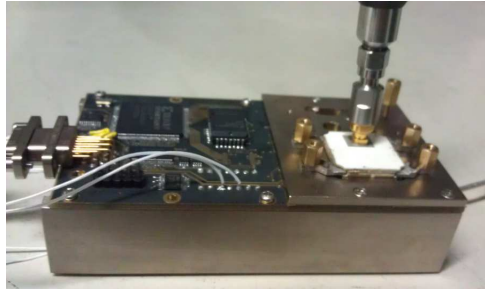


Figure 9. Test vehicle with LTCC T/R module.

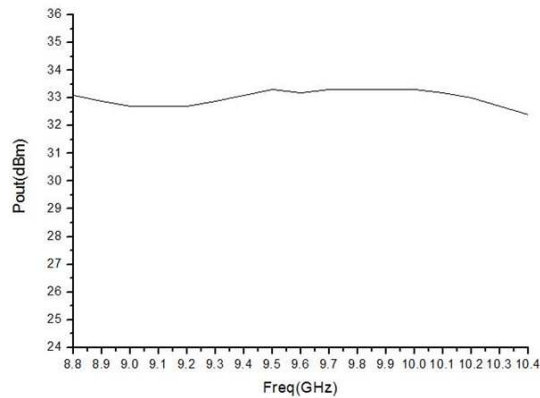


Figure 10. Output power in transmit mode.

through an attenuator. As shown in Figure 10, in the transmit mode, a measured output power of 33 ± 1 dBm is achieved in the frequency range from 8.8 GHz to 10.4 GHz. And in this circumstance the saturated input power is 12 dBm.

Measurements of gain and NF in receive mode are performed with Rohde & Schwarz ZVT20 Vector Network Analyzer and Agilent N8975A Noise Figure Analyzer, respectively. As shown in Figure 11, receive gain is about 30 dB and the smoothness is acceptable for the application. NF is 2.6–2.8 dB. According to the equation of cascade receive Noise Figure referred as (1), the loss of vertical interconnection (NF_1) of BGA has an obvious impact on the receive NF. Since the receive Noise Figure is less than 2.8 dB, it can be indicated that the loss of the vertical interconnection of BGA is small. Therefore, the presented T/R module prototype has been demonstrated and shows

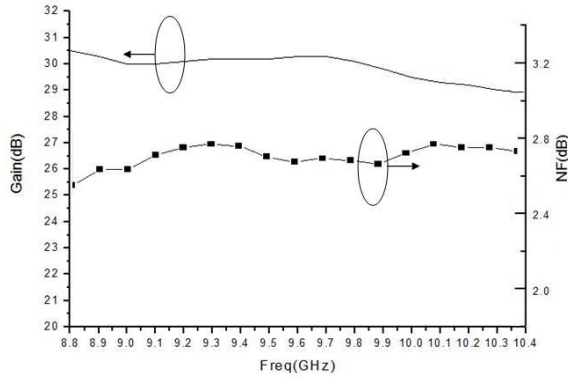


Figure 11. Gain and Noise Figure in receive mode.

good performance.

$$NF = NF_1 + \frac{NF_2 - 1}{G_1} + \frac{NF_3 - 1}{G_1 G_2} + \dots + \frac{NF_n - 1}{G_1 G_2 \dots G_{n-1}} \quad (1)$$

5. CONCLUSION

This paper has introduced an X-band tile T/R module prototype which operates at a frequency range of 8.8–10.4 GHz. Simulation of vertical interconnection methods involved has been performed, and a demonstrator has been realized and tested. An overall package solution benefiting from LTCC processes is adopted, which contributes to the reduction of size and weight of the module. The whole T/R module has a dimension of $20 \times 20 \times 2.6 \text{ mm}^3$, bearing a weight of 3.5 g. The tiny and compact module achieves high output power, receive gain and low noise. Test result indicates that it is feasible to adopt vertical interconnection with techniques detailed in this paper.

In the future work, when the mini-SMP and lid described in this paper are replaced with a patch antenna integrated into the lid, weight of the LTCC T/R module can be reduced further.

ACKNOWLEDGMENT

The authors would like to acknowledge the assistance and support of colleagues in Department of Space Microwave Remote Sensing System, IECAS.

REFERENCES

1. Hauhe, M. S. and J. J. Wooldridge, "High density packaging of X-band active array modules," *IEEE Transactions on Components, Packaging, and Manufacturing Technology*, Vol. 20, No. 3, 279–291, 1997.
2. Jantunen, H., T. Kangasvieri, J. Vähäkangas, and S. Leppävuori, "Design aspects of microwave components with LTCC technique," *Journal of the European Ceramic Society*, Vol. 23, No. 14, 2541–2548, 2003.
3. Mancuso, Y., "Components and technologies for T/R modules," *IEEE Aerospace and Electronic Systems Magazine*, Vol. 25, No. 10, 39–43, 2010.
4. Wang, Z., P. Li, R. M. Xu, and W. Lin, "A compact X-band receiver front-end module based on low temperature co-fired ceramic technology," *Progress In Electromagnetics Research*, Vol. 92, 167–180, 2009.
5. Thorsell, M., M. Fagerlind, K. Andersson, N. Billstrom, and N. Rorsman, "An X-band AlGaIn/GaN MMIC receiver front-end," *IEEE Microwave and Wireless Components Letters*, Vol. 20, No. 1, 55–57, 2010.
6. Donelli, M. and P. Febvre, "An inexpensive reconfigurable planar array for Wi-Fi applications," *Progress In Electromagnetics Research C*, Vol. 28, 71–81, 2012.
7. Donelli, M., R. Azaro, L. Fimognari, et al., "A planar electronically reconfigurable Wi-Fi band antenna based on a parasitic microstrip structure," *IEEE Antennas and Wireless Propagation Letters*, Vol. 6, 623–626, 2007.
8. Donelli, M., "A rescue radar system for the detection of victims trapped under rubble based on the independent component analysis algorithm," *Progress In Electromagnetics Research M*, Vol. 19, 173–181, 2011.
9. Rosenberger GmbH, "Mini SMP straight plug PCB full detent," 2011, Available: <http://rosenberger.de/ok/images/documents/db/18S101-40ML5.pdf>.
10. Pillai, E. R., "Coax via-A technique to reduce crosstalk and enhance impedance match at vias in high-frequency multilayer packages verified by FDTD and MoM modeling," *IEEE Trans. Microwave Theory and Tech.*, Vol. 45, No. 10, 1981–1985, 1997.
11. Darwish, A., A. Ezzeddine, H. C. Huang, et al., "Analysis of three-dimensional embedded transmission lines (ETL's)," *IEEE*

- Microwave and Guided Wave Letters*, Vol. 9, No. 11, 447–449, 1999.
12. Machado, A. G., D. V. Martin, A. A. Lopez, and J. G. Menoyo, “Microstrip-to-stripline planar transitions on LTCC,” *IEEE MTT-S Microwave Workshop Series on Millimeter Wave Integration Technologies*, 1–4, 2011.
 13. Kim, G., A. C. W. Lu, F. Wei, L. L. Wai, and J. Kim, “3D strip meander delay line structure for multilayer LTCC-based SIP applications,” *Electronic Components and Technology Conference*, 2081–2085, 2008.
 14. Schreiner, M., H. Leier, W. Menzel, and H. P. Feldle, “Architecture and interconnect technologies for a novel conformal active phased array radar module,” *IEEE MTT-S Microwave Symposium Digest*, 567–570, 2003.